

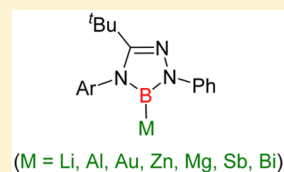
# Isolation of 1,2,4,3-Triazaborol-3-yl-metal (Li, Mg, Al, Au, Zn, Sb, Bi) Derivatives and Reactivity toward CO and Isonitriles

Wei Lu,<sup>†</sup> Haitao Hu,<sup>†</sup> Yongxin Li,<sup>‡</sup> Rakesh Ganguly,<sup>‡</sup> and Rei Kinjo<sup>\*,†</sup>

<sup>†</sup>Division of Chemistry and Biological Chemistry, School of Physical and Mathematical Sciences and <sup>‡</sup>NTU-CBC Crystallography Facility, Nanyang Technological University, 637371, Singapore

**S** Supporting Information

**ABSTRACT:** 3,4-dihydro-2*H*-1,2,4,3-triazaborol-3-yl-lithium **3** was synthesized and fully characterized. The <sup>11</sup>B NMR spectrum, X-ray diffraction analysis, and computational studies revealed the ionic nature of the B–Li bond, and indeed **3** displays nucleophilic property which allowed preparation of a series of 1,2,4,3-triazaborol-3-yl-metal complexes (Al; **5**, Au; **6**, Zn; **7**, Mg; **8**, Sb; **9**, and Bi; **10**). **3** reacted with CO (1 atm) and various isocyanides under ambient condition, and mechanistic study suggests that the reactions with CO and aryl isocyanides proceed via an insertion of CO and isocyanide carbon into the B–Li bond followed by isomerization to yield transient carbene species, one of which was confirmed by trapping with S<sub>8</sub>. With PhNC, compounds **5** and **7**·(thf) underwent exchange of THF molecule coordinating to the metal center with isocyanide, whereas insertion of isocyanide carbon occurred at the B–Bi bond in **10** which afforded stable bismuth (boryl)iminomethane **20**.



## INTRODUCTION

Borylmetals are widely involved as key intermediates in the plethora of organometallic processes, ranging from classical metal-catalyzed hydroboration and diboration to recent dehydrogenative borylation.<sup>1</sup> Accordingly, a deep comprehension of the intrinsic property of the B–M bond is essential to developing the realm. As such, considerable efforts have been made for the isolation of borylmetals over the past decade. In 2006, Nozaki and Yamashita et al. first reported a bottleable boryllithium (DAB)BLi (DAB = {DippNCH}<sub>2</sub>, Dipp = 2,6-diisopropylphenyl) **I** (Figure 1),<sup>2</sup> which opened up synthetic routes to other borylmetals.<sup>3</sup> Indeed, the same group described the preparation and structural characterization of other boryllithiums **II** and **III**<sup>4</sup> as well as borylmagnesium **IV**,<sup>5</sup> borylzinc **V**,<sup>6a</sup> borylcopper compounds **VI** and **VII** (Figure 1)<sup>6</sup> and demonstrated the nucleophilic nature of these molecules. Since this pivotal work, several groups have developed other systems involving nucleophilic boron center such as N-heterocyclic carbene-stabilized π-boryl anion **VIII**,<sup>7</sup> borylcopper complex **IX**,<sup>8</sup> anionic dimetalloborylene **X**,<sup>9</sup> tricyanoborate dianion **XI**,<sup>10</sup> and cyclic (alkyl) (amino)carbene-supported dicyanoborate monoanion **XII**.<sup>11</sup> Isolation of **I–XII** has brought significant advances in organoboron, organometallic, and synthetic chemistry.<sup>12</sup> However, most of the nucleophilic boryl metals utilized in those literatures are composed of the BC<sub>2</sub>N<sub>2</sub> five-membered ring, particularly, **I**.<sup>3,12</sup> This is mainly because of: (i) the ease of synthetic access: two steps starting from commercially available BBr<sub>3</sub> and 1,2-bis(2,6-diisopropylphenylimino)ethane,<sup>2,4</sup> (ii) the robustness owing to the rigid ring system as well as effective interaction between the unoccupied p-orbital of the B atom and the lone pair electrons on the N atoms, and (iii) effective steric impact at the B center by the Ar groups on the N atoms, allowing for a kinetic stabilization of the resulting B–E bond in the

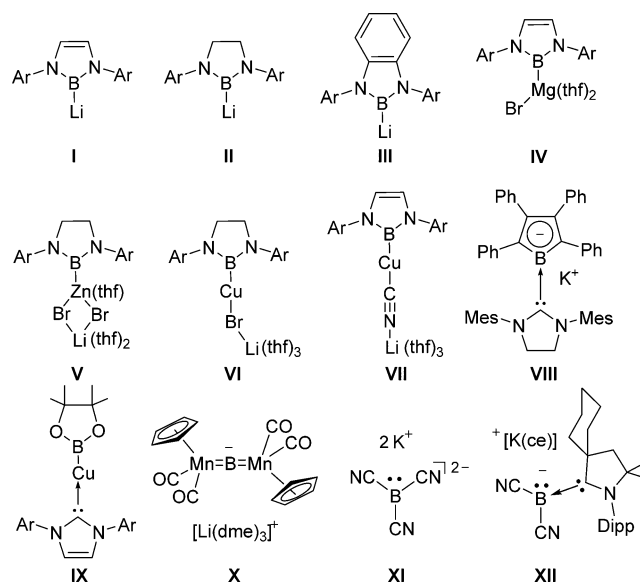


**Figure 1.** Structurally characterized borylmetals and related anionic and/or nucleophilic boron-containing species **I–XII**.

products.<sup>13</sup> Given the advantages of the five-membered ring system, modulation of the five-membered ring skeleton will expand the diversity of borylmetal chemistry. Nevertheless, five-membered ring systems involving the B–M bond, other than the BC<sub>2</sub>N<sub>2</sub> ring type such as **I–VII** and pinacol borane type **IX**, have never been described thus far, which prompted us to extend the borylmetal family based on hitherto unknown five-membered ring framework. Herein, we report isolation of

Received: April 4, 2016

Published: May 2, 2016

1,2,4,3-triazaborol-3-yl-lithium and other borylmetals. We also show systematic and comparative studies on the reactivity of these borylmetals to carbon monoxide and isonitrile derivatives.

## RESULTS AND DISCUSSION

**Syntheses and Structures of 1,2,4,3-Triazaborol-3-yl-lithium and Other Metal (Al, Au, Zn, Mg, Sb, and Bi) Derivatives.** In carbene chemistry, it has been demonstrated that by replacing one of the skeletal carbon atoms of classical N-heterocyclic carbenes with a nitrogen atom, the intrinsic electronic feature of the carbene center can be modulated (Figure 2, A and B).<sup>14</sup> Due to the similar structural relationship

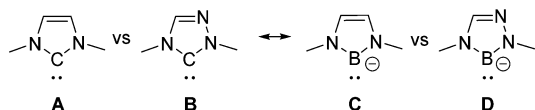
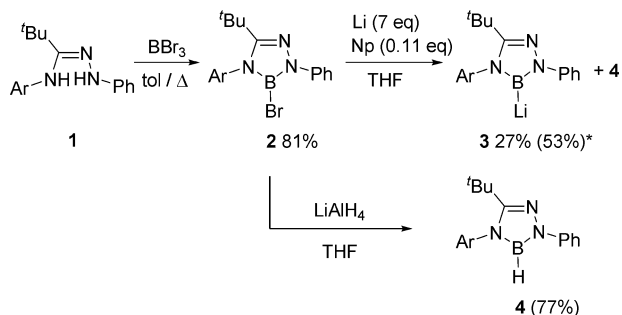


**Figure 2.** Structural relationship between N-heterocyclic carbenes A and B and boryl anions C and D.

between carbenes  $A \leftrightarrow B$  and boryl anions  $C \leftrightarrow D$ , we were interested to investigate the chemical property of boryl anion D. 1,2,4,3-Triazaborole derivative **2** was synthesized by the reaction of amidrazone **1**<sup>15</sup> and  $BBr_3$  in toluene under reflux condition. Compound **2** was fully characterized by standard spectroscopic methods and X-ray diffraction analysis. Treatment of **2** with excess amounts of lithium in the presence of naphthalene (11.5 mol %) in tetrahydrofuran (THF) at  $-78^\circ C$  afforded a red solution. After workup, boryl lithium **3** was isolated as a red solid in 27% yield (Scheme 1). We also

### Scheme 1. Synthesis of **2** and **3**<sup>a</sup>



<sup>a</sup>Ar = 2,6-diisopropyl-phenyl; Np = naphthalene. \* indicates NMR yield.

checked the NMR yield (53%), using 1,3,5-trimethoxybenzene as an internal standard. The moderate yield is due to the formation of a byproduct, assigned to B-protonated species **4**, which was decisively confirmed by independent reaction between **2** and  $LiAlH_4$  (Scheme 1). Except for **4**, we also detected trace amounts of signals for unidentified byproducts. In the  $^{11}B$  NMR spectrum of **3**, a broad singlet appears at 47.9 ppm ( $\nu_{1/2} = 811$  Hz), which is slightly shifted downfield with respect to that of **1** (45.4 ppm in THF- $d_8$ ). Single crystals of **3** were obtained by recrystallization from pentane at  $-20^\circ C$ , and X-ray diffraction study revealed that the boron atom directly bonds to the lithium atom (Figure 3). The Li atom is coordinated by three THF molecules, which is contrast to Nozaki and Yamashita's boryllithiums where lithium is coordinated by only two THF molecules.<sup>2,4</sup> All five atoms of the  $BCN_3$  ring are coplanar with the sum of internal pentagon

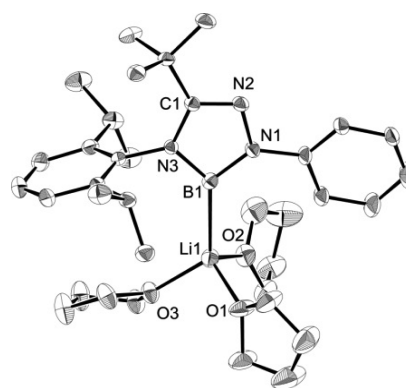
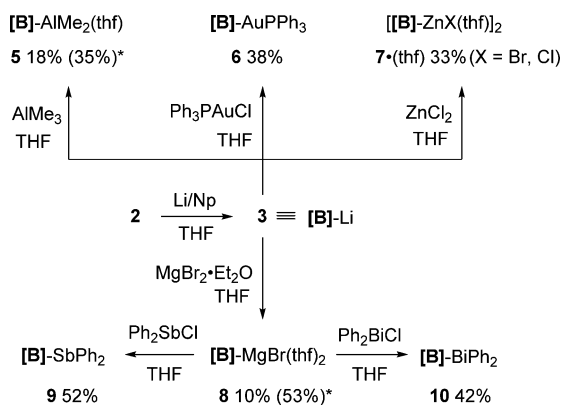


**Figure 3.** Solid-state structure of  $3 \cdot (thf)_3$  (all hydrogen atoms are omitted for clarity). Thermal ellipsoids are set at the 50% probability level.

angles of  $540.00^\circ$ . Phenyl ring at N1 and the  $BCN_3$  five-membered ring are slightly twisted by  $14.6^\circ$ , whereas the 2,6- $^iPr_2C_6H_3$ -group at N3 and the  $BCN_3$  skeleton are nearly perpendicular to each other with the twist angle of  $87.9^\circ$ . The N1–B1–N3 bond angle is  $96.8(2)^\circ$  which is smaller than that ( $105.4(3)^\circ$ ) of **2**. The B1–Li1 distance of  $2.343(5)$  Å is 11.0% longer than the sum of the covalent radii ( $2.11$  Å)<sup>16</sup> and significantly longer than those ( $2.218(9)$ – $2.291(6)$  Å) of boryllithiums I–III.<sup>2,4</sup> The two B–N bond lengths ( $1.462(4)$  Å and  $1.484(3)$  Å) are similar to those ( $1.474(3)$  Å and  $1.480(4)$  Å) observed in I·(thf)<sub>2</sub>. Note that **3** is the first isolable 1,2,4,3-triazaborol-3-yl-lithium.

Having new boryllithium **3** in hand, next we examined the preparation of several borylmetals. Boryllithium **3** was generated in situ and subsequently treated with metal precursors (Scheme 2). With excess  $AlMe_3$  in THF, [B]-

### Scheme 2. Synthesis of Borylmetal Derivatives **5**–**10**<sup>a</sup>



<sup>a</sup>\* indicates NMR yield.

$AlMe_2(thf)$  **5** was obtained as a colorless solid in 18% isolated yield, concomitant with the formation of  $LiAlMe_4$  as a byproduct. The  $^{11}B\{^1H\}$  NMR spectra of **5** shows a peak at 33.1 ppm, while the  $^{27}Al$  NMR chemical shift appears at 69.6 ppm; these are comparable to those ( $^{11}B$ : 31.9 ppm;  $^{27}Al$ : 68.7 ppm) of (DAB)B- $AlMe_2(thf)$  reported by Anwander and co-workers.<sup>3a</sup>

Treatment of **3** with a stoichiometric amount of  $(Ph_3P)AuCl$  afforded  $Ph_3P$ -borylgold complex **6** in 38% yield. The  $^{11}B\{^1H\}$  NMR spectra of **6** display a singlet at 48.7 ppm, which is slightly shifted downfield with respect to that (45.4 ppm) of

(DAB)B-AuPPh<sub>3</sub> developed by Nozaki and Yamashita et al.<sup>3h</sup> In the <sup>31</sup>P NMR spectrum of **6**, a phosphorus resonance was observed at 57.0 ppm, identical to that (57.7 ppm) of (DAB)B-AuPPh<sub>3</sub>. Transmetalation of **3** with 1 equiv of ZnCl<sub>2</sub> in THF proceeded smoothly, and borylhalozinc species **7**·(thf) was isolated in 33% yield after workup. In the <sup>11</sup>B NMR spectrum, a broad peak appeared at 34.4 ppm, which is shifted upfield compared with that (41 ppm) of lithium boryldibromozincate (L)B-Zn(thf)Br<sub>2</sub>Li(thf)<sub>2</sub> **V** (L = {DippNCH<sub>2</sub>})<sub>2</sub> and that (38 ppm) of [(DAB)<sub>2</sub>Zn], and comparable to that (32 ppm) of diborylzinc species [(L)B]<sub>2</sub>Zn.<sup>6</sup> Similarly, transmetalation of **3** with MgBr<sub>2</sub>·Et<sub>2</sub>O in THF afforded the corresponding borylmagnesium **8** in 10% isolated yield. The <sup>11</sup>B NMR signal appears as a broad singlet at 38.7 ppm, which is close to the reported values (~37.6 ppm) for (DAB)B-MgBr(thf)<sub>2</sub> **IV**, (DAB)B-Mg(thf)Br<sub>2</sub>Li(thf)<sub>2</sub>, and [(DAB)B]<sub>2</sub>Mg(thf)<sub>2</sub>.<sup>5</sup> These results demonstrate that compound **3** displays nucleophilic nature toward metal-halides, which encouraged us to examine the preparation of hitherto unexplored boryl-group 15 metal compounds. Recently, Jones and co-workers reported that the reaction of L'BiBr<sub>2</sub> (L' = ArNSiMe<sub>3</sub>) with 2 equiv of **I** gave diboryldibismuthene (DAB)B-Bi = Bi-B(DAB), while the reaction of BiBr<sub>3</sub> with **I** gave rise to bismuth metal deposition concomitant with the formation of BrB(DAB).<sup>17</sup> Similarly, when we treated compound **3** with SbCl<sub>3</sub> or BiCl<sub>3</sub>, a black precipitate appeared immediately, and only a complex mixture involving **2** was observed in the NMR spectra. We reasoned that employment of borylmagnesium **8**, much weaker reducing reagent than **3**, may inhibit electron-transfer process, which will allow nucleophilic substitution along with MgX<sub>2</sub>-salt elimination. To bear out the hypothesis, borylmagnesium **8** was reacted with 1 equiv of Ph<sub>2</sub>SbCl or Ph<sub>2</sub>BiCl, which afforded boryldiphenylstibane **9** and boryldiphenylbismuthane **10** in 52% and 42% yields, respectively. The <sup>11</sup>B NMR spectra of **9** and **10** showed signal at 30.9 and 50.6 ppm, respectively.

The structures of borylmetals **5–10** were unambiguously determined by X-ray crystallography (Figures 4–9). In the

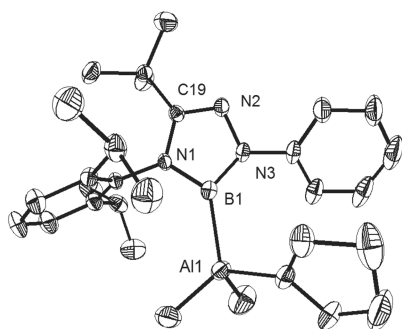


**Figure 4.** Solid-state structure of **5** (all hydrogen atoms are omitted for clarity). Thermal ellipsoids are set at the 50% probability level.

solid-state structure of **5** (Figure 4), the Al center is tetra-coordinate with the boryl group, two methyl groups, and a THF molecule. The distances of B1–Al1 bond [2.155(2) Å], the Al1–C bonds [1.974(2) Å and 1.985(2) Å], and Al1–O1 bond [1.946(2) Å] are comparable to those [B–Al: 2.150(2) Å, Al–C: 1.974(2) Å, and 1.981(2) Å, Al–O: 1.940(2) Å] of (DAB)B-AlMe<sub>2</sub>(thf).<sup>3a</sup> The B1–Al1–C bond angles [117.71(9)° and 117.52(11)°] are nearly identical to those [115.34(9)° and 117.87(9)°] in (DAB)B-AlMe<sub>2</sub>(thf), whereas

the B1–Al1–O1 bond angles of 101.63(7)° are slightly smaller than that [106.26(8)°] in (DAB)B-AlMe<sub>2</sub>(thf).

Compound **6** involves both boryl and Ph<sub>3</sub>P ligands coordinating to the Au(I) center in linear fashion, and the B1–Au1–P1 angle [172.21(9)°] deviates slightly from linearity (Figure 5). The B1–Au1 distance of 2.069(3) Å is close to that

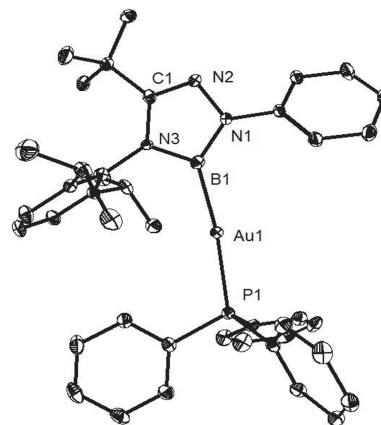


**Figure 5.** Solid-state structure of **6** (all hydrogen atoms are omitted for clarity). Thermal ellipsoids are set at the 50% probability level.

[2.076(6) Å] in (DAB)B-AuPPh<sub>3</sub><sup>3h</sup> and, thus, in agreement with the formation of 2c-2e B–Au bond. The P1–Au1 distance of 2.341(1) Å is longer than those [2.235(3) ~ 2.296(2) Å] in Ph<sub>3</sub>PAuX (X = Cl, Me, Ph) derivatives,<sup>18</sup> supporting the strong trans influence of the boryl ligand.

Colorless single crystals were grown from a saturated acetonitrile solution at ambient temperature, and the solid-state molecular structure of **7**·(MeCN) revealed that **7**·(MeCN) co-crystallizes as a mixture of various amount of borylchlorozinc **7**-Cl and borylbromozinc **7**-Br species. For the structure shown in Figure 6, 67% of **7**-Br is present. Both

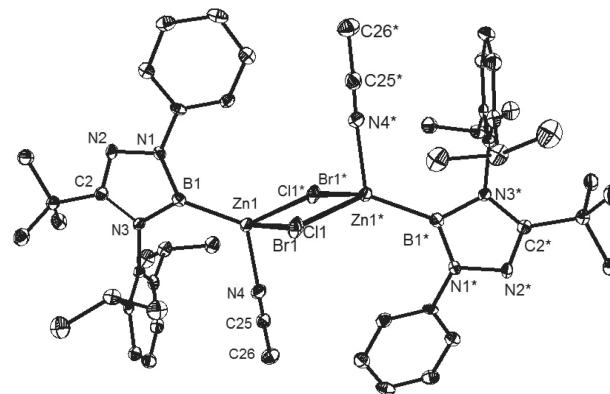


**Figure 6.** Solid-state structure of **7**·(MeCN) (all hydrogen atoms are omitted for clarity). Thermal ellipsoids are set at the 50% probability level.

compounds were refined with the ratio of occupancy **7**-Cl/**7**-Br equal to 33/67. **7**-Br was presumably produced via halogen exchange of **7**-Cl by LiBr which was formed during the generation of **3**. Compound **7**·(MeCN) presents the first geometric example displaying dimeric form of [B]-ZnX·(MeCN), which is in sharp contrast to the structure of lithium boryldibromozincate (L)B-Zn(thf)Br<sub>2</sub>Li(thf)<sub>2</sub> **V**.<sup>6</sup> The [B]-Zn(MeCN) moieties in the structure of **7**-Cl and **7**-Br are

absolutely identical. The zinc atom is tetra-coordinate with boryl ligand, acetonitrile molecule, and two halogen atoms. The B1–Zn1 bond length [2.066(3) Å] is slightly shorter than that [2.0755(5) Å] of (L)B–Zn(thf)Br<sub>2</sub>Li(thf)<sub>2</sub> and those [2.088(3) Å and 2.087(3) Å] in (L)B–Zn–B(L), but longer than those [2.052(3) Å and 2.053(3) Å] in (DAB)B–Zn–B(DAB).<sup>6</sup>

In the crystal structure of **8**, the sp<sup>3</sup> Mg center is coordinated by the boryl group, a Br atom, and two THF molecules (Figure 7). The B1–Mg1 distance [2.341(7) Å] is longer than the sum

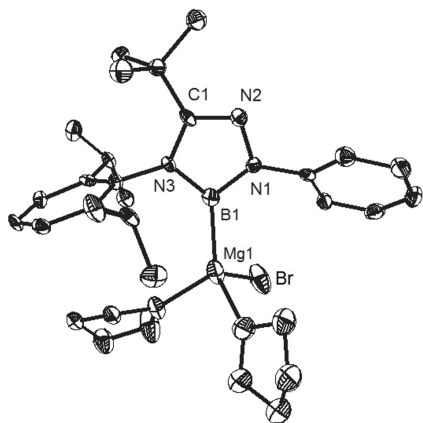


**Figure 7.** Solid-state structure of **8** (all hydrogen atoms are omitted for clarity). Thermal ellipsoids are set at the 50% probability level.

(2.24 Å) of covalent radii of B and Mg atoms and 0.06 Å longer than that [2.281(6) Å] in (DAB)B–MgBr(thf)<sub>2</sub> **IV**,<sup>5</sup> supporting an ionic nature of the B–Mg bond.

Figure 8 shows the molecular structure of **9** with a rare example of structurally characterized B–Sb single bond.<sup>19</sup> The

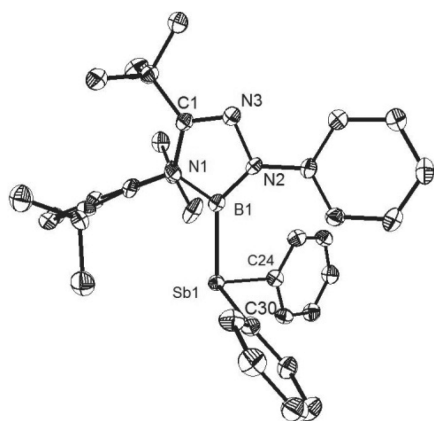


**Figure 8.** Solid-state structure of **9** (all hydrogen atoms are omitted for clarity). Thermal ellipsoids are set at the 50% probability level.

B–Sb distance of 2.257(5) Å is nearly identical to the sum (2.25 Å) of covalent radii of B and Sb atoms and 0.06 Å shorter than that [2.318(2) Å] in Scheer's parent stibanylborane H<sub>2</sub>SbBH<sub>2</sub>·(NHC<sup>Me</sup>) featuring a 2-center-2-electron Sb–B  $\sigma$ -bond.<sup>20</sup> The Sb–C distances [2.157(4) Å and 2.173(4) Å] are comparable to that [2.155(9) Å] in SbPh<sub>3</sub>.<sup>21</sup> The B1–Sb1–C bond angles [98.49(17)° and 100.65(16)°] and the C24–Sb1–C30 bond angle [100.25(16)°] are similar (sum of the bond angles: 299.39°), and the magnitudes of these bond angles indicate a high p-character of the bonds and, thus, a high s-character to the Sb lone pair electrons. Similar geometric

property was observed in the structure of **10** (Figure 9). The B–Bi distance of 2.343(6) Å is close to the sum (2.32 Å) of

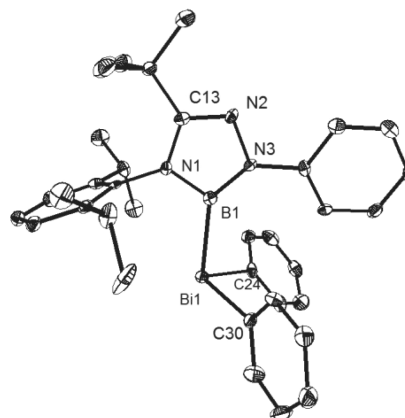


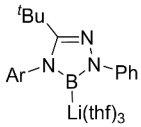
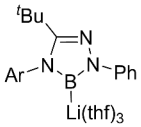
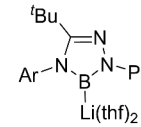
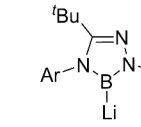
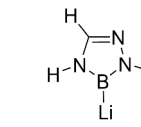
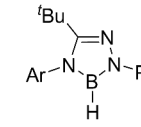
**Figure 9.** Solid-state structure of **10** (all hydrogen atoms are omitted for clarity). Thermal ellipsoids are set at the 50% probability level.

covalent radii of B and Bi atoms as well as those [2.326(7) Å and 2.317(9) Å] in (DAB)B–Bi = Bi–B(DAB).<sup>17</sup> The B1–Bi1–C bond angles [96.65(19)° and 99.41(18)°] are similar to the C24–Bi1–C30 bond angle [98.42(18)°] (sum of the bond angles: 294.48°).

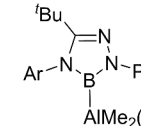
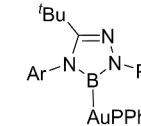
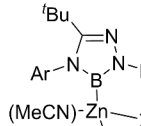
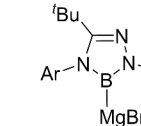
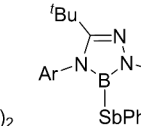
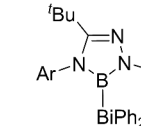
The selected metric parameters and the <sup>11</sup>B NMR chemical shifts of compounds **3–10** are summarized in Table 1, with those of computationally optimized molecules: **opt-3**·(thf)<sub>3</sub>, **opt-3**·(thf)<sub>2</sub>, **opt-3**, **opt-3'**. The B–N bond distances [1.462(4) and 1.484(3) Å in 3·(thf)<sub>3</sub>; 1.434(2) and 1.460(2) Å in **5**; 1.431(4) and 1.453(4) Å in **6**; 1.435(4) and 1.454(4) Å in 7·(MeCN); 1.449(7) and 1.477(8) Å in **8**; 1.434(6) and 1.437(6) Å in **9**; 1.416(7) and 1.432(7) Å in **10**] are longer than those [1.402(3) and 1.411(3) Å] in hydroborane **4**. In addition, the N–B–N bond angles [96.8(2)° in 3·(thf)<sub>3</sub>; 99.87(14)° in **5**; 101.3(3)° in **6**; 100.8(2)° in 7·(MeCN); 98.7(5)° in **8**; 103.0(4)° in **9**; 103.8(2)° in **10**] are smaller than that [104.7(2)°] in **4**. Similar geometric relationships were reported between borylmetals (DAB)B–M and its hydroborane (DAB)B–H<sup>2–4</sup> as well as N-heterocyclic carbenes and imidazolium salts,<sup>22</sup> which supports ionic character of the boron–metal bonds in compounds **3–10**. Structural parameters of calculated compounds **opt-3**·(thf)<sub>3</sub> and **opt-3**·(thf)<sub>2</sub> well agreed with the experimental results, and the metric parameters of **opt-3** and **opt-3'** indicate that absence of THF molecules on the Li atom increases covalent property of the B–Li bond along with shortening of the B–Li bond and widening of the N–B–N bond angle. The calculated <sup>11</sup>B NMR chemical shift for **opt-3**·(thf)<sub>3</sub> ( $\delta_B$  46.5) rather than **opt-3**·(thf)<sub>2</sub> ( $\delta_B$  43.8) is close to the experimentally observed value ( $\delta_B$  47.9), and the chemical shift for THF-free compound **opt-3** ( $\delta_B$  40.6) is far from the experimental value. These data suggest that in a THF solution, the Li atom in **3** is surrounded by several THF molecules, thus **3** may be present in 3·(thf)<sub>n</sub> fashion rather than the THF-free form.

**Electronic Structure of Boryllithium 3.** To elucidate the electronic property of boryllithium **3**, we carried out further analysis of the electronic property using DFT calculations. Figure 10 illustrates the HOMOs of **opt-3**·(thf)<sub>3</sub> and **opt-3'**. NPA charges of **opt-3'** and the parent derivative of (DAB)BLi **opt-1'** are given in Figure 11. The HOMOs of both of **opt-3**·(thf)<sub>3</sub> and **opt-3'** are almost identical and display mainly the

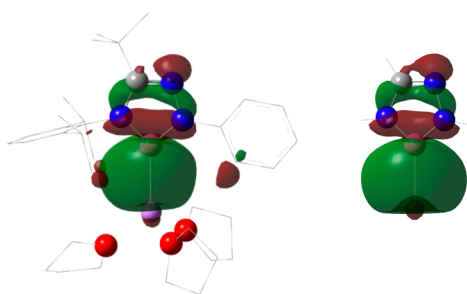
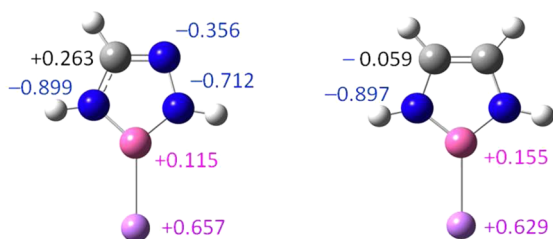
Table 1. Selected Structural Parameters and  $^{11}\text{B}$  NMR Chemical Shifts of 3–10 and Calculated Compounds

						
(Ar = 2,6- $i$ -Pr <sub>2</sub> C <sub>6</sub> H <sub>3</sub> )	<b>3(thf)<sub>3</sub></b>	<b>opt-3•(thf)<sub>3</sub><sup>a</sup></b>	<b>opt-3•(thf)<sub>2</sub><sup>a</sup></b>	<b>opt-3<sup>a</sup></b>	<b>opt-3'<sup>a</sup></b>	<b>4</b>
B-M (Å)	2.343(5)	2.414(8)	2.310	2.204	2.222	-
B-N (Å)	1.462(4)	1.465(1)	1.451	1.437	1.430	1.402(3)
B-N (Å)	1.484(3)	1.490(1)	1.484	1.469	1.459	1.411(3)
N-B-N (°)	96.8(2)	97.3(9)	97.89	99.36	98.22	104.7(2)
$\delta_{\text{B}}$ (ppm)	47.9	46.5 <sup>b</sup>	43.8 <sup>b</sup>	40.6 <sup>b</sup>	-	23.9

						
	<b>5</b>	<b>6</b>	<b>7•(MeCN)</b>	<b>8</b>	<b>9</b>	<b>10</b>
B-M (Å)	2.155(2)	2.069(3)	2.066(3)	2.341(7)	2.257(5)	2.343(6)
B-N (Å)	1.434(2)	1.431(4)	1.435(4)	1.449(7)	1.434(6)	1.416(7)
B-N (Å)	1.460(2)	1.453(4)	1.454(4)	1.477(8)	1.437(6)	1.432(7)
N-B-N (°)	99.87(14)	101.3(3)	100.8(2)	98.7(5)	103.0(4)	103.8(4)
$\delta_{\text{B}}$ (ppm)	33.1	48.7	34.4	38.7	30.9	50.6

<sup>a</sup>Calculated at HF/6-311+G(d, p) level of theory. <sup>b</sup>GIAO/ $^{11}\text{B}$  NMR were performed at B3LYP/6-311+G(d, p) level of theory.

Figure 10. HOMOs of **opt-3**•(thf)<sub>3</sub> (left) and **opt-3'** (right).Figure 11. NPA charges of the BCN<sub>3</sub> five-membered ring in **opt-3'** (left) and **opt-I'** (right).

B–Li  $\sigma$ -bonding orbitals, indicating that substitution at the BCN<sub>3</sub> five-membered skeleton and coordination of THF molecules to the Li atom do not affect the shape of the HOMO. Meanwhile, NPA charges of **opt-3'** and **opt-I'** suggest that the presence of an additional N atom in the five-membered ring essentially affect the property of the B–Li bonds. Thus, the B atom ( $q_{\text{B}} + 0.115$ ) in **opt-3'** is less positive than that ( $q_{\text{B}} + 0.155$ ) in **opt-I'**, and consequently, the ionic nature of the B–Li bond ( $\Delta q_{\text{B-Li}} = 0.542$ ) in **opt-3'** is greater than that ( $\Delta q_{\text{B-Li}} = 0.474$ ) in **opt-I'**. Natural bond orbital (NBO) analysis gave Wiberg bond index (WBI) values smaller than 1 for the B–Li

bond (0.55 for **opt-3'**, 0.58 for **opt-I'**), which is in line with the ionic property of the B–Li bond.

#### Electronic Structures of Compounds 9 and 10.

Compounds 9 and 10 represent very rare examples of molecules bearing group 15 metal–boron bonds.<sup>17,19,20</sup> To gain deep insight into the electronic property of group 15 metal–boron bonds, we performed a molecular orbital (MO) analysis and NBO analysis. The metal–boron bonding interactions were found in the HOMO of 9 and the HOMO–1 of 10, respectively (Figure 12). Both MOs

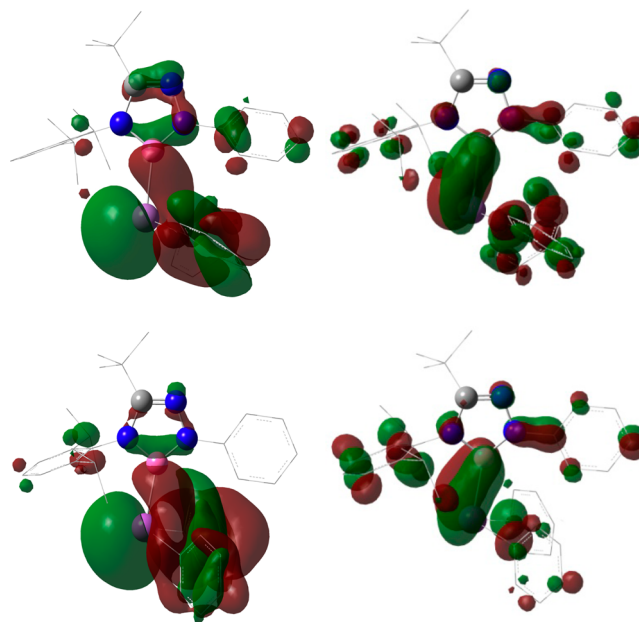
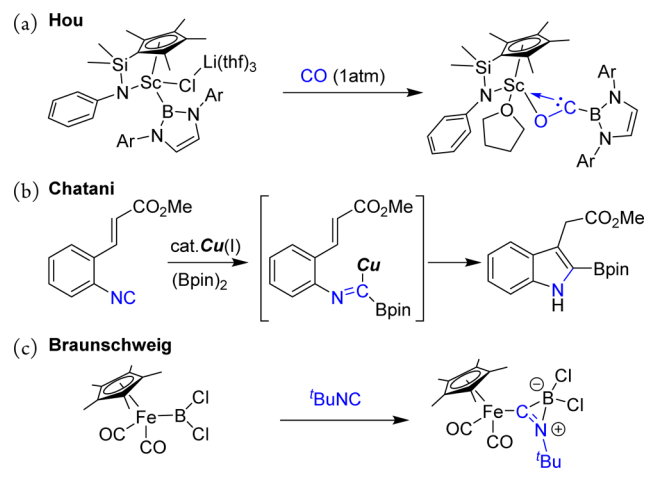


Figure 12. Plots of the HOMO (top left) and LUMO (top right) of 9 (top right), and the HOMO–1 (bottom left) and LUMO (bottom right) of 10.

displaying similar shapes involve the lone pair orbital of the metal with some contribution from  $\pi$ -orbitals of Ph-groups substituted on the metal. Meanwhile, the LUMOs of **9** and **10** are mainly  $\pi$ -type orbitals spreading over the B atom and the metal (Sb, Bi). NBO analysis gave WBI values for the B1–Sb1 bond (0.95) in **9** and the B1–Bi1 (0.94) in **10** and revealed that these bonds are formed from the high-p-character hybrid orbital of the metal atom (Sb in **9**:  $s = 15.67\%$ ,  $p = 84.33\%$ , Bi in **10**:  $s = 11.21\%$ ,  $p = 88.70\%$ ) and the s-p mixed orbital of the B atom (B in **9**:  $s = 42.00\%$ ,  $p = 57.93\%$ , B in **10**:  $s = 43.92\%$ ,  $p = 56.02\%$ ). We also estimated the bond dissociation energies (BDEs) for hemolytic cleavage of the M–B bonds in **9** and **10**. The calculated BDEs for the Sb–B bond ( $121 \text{ kJ}\cdot\text{mol}^{-1}$ ) in **9** and the Bi–B bond ( $91 \text{ kJ}\cdot\text{mol}^{-1}$ ) in **10** are significantly smaller than those (Sb–B  $264 \text{ kJ}\cdot\text{mol}^{-1}$ , Bi–B  $234 \text{ kJ}\cdot\text{mol}^{-1}$ ) estimated for  $\text{H}_2\text{M}\cdot\text{BH}_2$ ,<sup>20</sup> which is presumably, in part, due to steric repulsion between bulky boryl ligand and diphenyl-substituted metals as well as a stabilization of metal radical species by two phenyl groups.

**Reactivity of 1,2,4,3-Triazaborol-3-yl-lithium **3** toward Carbon Monoxide and Isonitriles.** Insertion reaction of carbon monoxide (CO), an industrial  $\text{C}_1$  building block, into the carbon–lithium bond in organolithium reagents is of significant importance in organic synthesis due to the potential applications of carbonyllithium species which could be the initial intermediate of the reaction, for the various carbonylative reactions.<sup>23</sup> Meanwhile, the corresponding insertion of gaseous CO into the boron–metal bond has been little studied.<sup>24</sup> Recently, Hou and co-workers reported the reaction of CO with borylscandium complex in which insertion of CO to the Sc–B bond afforded an isolable (boryl) (oxy)carbene scandium complex (Scheme 3a).<sup>25</sup> Analogous to CO, isocyanides are useful

### Scheme 3. Reported Examples for Insertion of CO and Isonitriles into the Boron–Metal Bonds

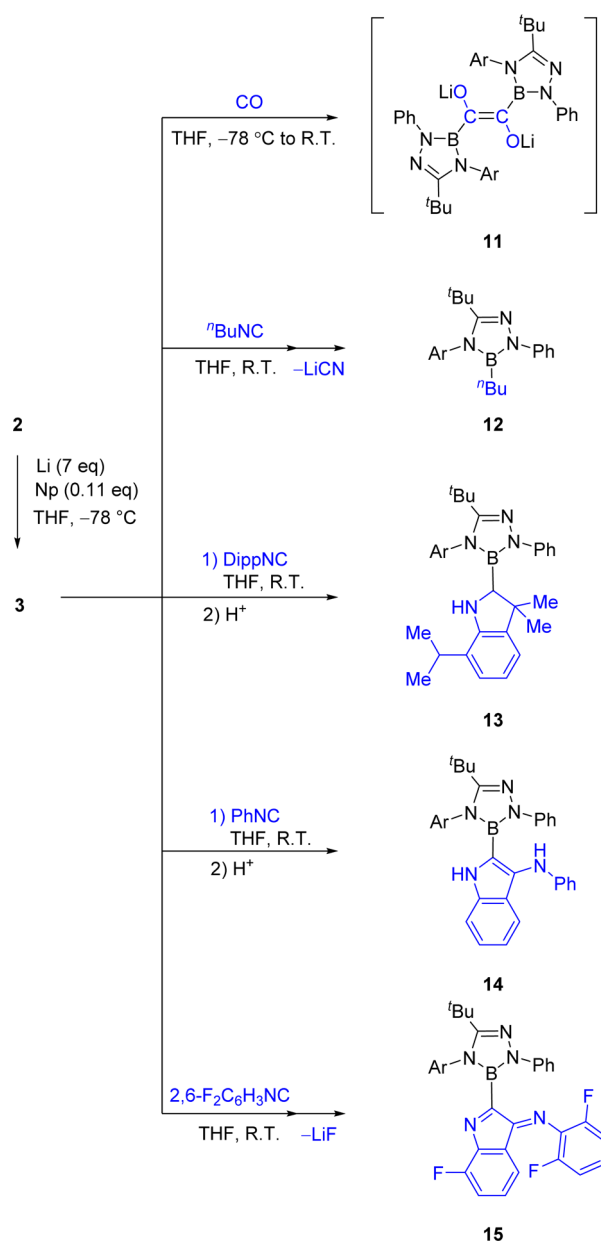


synthetic building blocks in organic chemistry as they extensively react with various substrates such as electrophiles, nucleophiles, and radicals.<sup>26</sup> Several groups reported that isocyanides inserted into the bonds between boron and nonmetal atoms (H, B, Si, and halogenes).<sup>27</sup> It has also been demonstrated that isocyanides reacted with borylene and metaloborylene (Fe, Cr and Mn) complexes via insertion of the isocyanide carbon into the B–M bond.<sup>28</sup> In contrast, the reaction of isocyanides with the  $\text{B}(\text{sp}^2)\text{--M}$   $\sigma$  bonds in borylmetals remains poorly investigated. In copper-catalyzed

borylative cyclization of 2-alkenylphenyl isocyanides, Chatani et al. proposed a mechanism involving isonitile insertion into the pinB–Cu bond in transient borylcopper intermediate (Scheme 3b).<sup>29</sup> Braunschweig and co-workers showed that activation of iron dichloroboryl complex by  $t\text{BuNC}$  resulted in the formation of a BCN three-membered ring (Scheme 3c).<sup>30</sup> While these pioneering studies indicate the potential utility of the B–M bonds insertion reaction because both the B–C( $\text{sp}^2$ ) and M–C( $\text{sp}^2$ ) bonds in the product are in principle functionalizable, as far as we are aware, the reactions of boryllithium with CO and isocyanides have never been studied thus far, which motivated us to investigate the reactions of **3** and other borylmetals with CO and isocyanides.

First, we examined the reactivity of boryllithium **3** toward carbon monoxide and various isocyanides (Scheme 4). Treatment of a THF solution of boryllithium **3** freshly generated *in situ* with CO (1 atm) led to a deep pink solution. The  $^{11}\text{B}$

### Scheme 4. Reactions of **3** with CO and Isonitriles



NMR of the reaction mixture displayed a broad singlet at 30.1 ppm, which could correspond to 1,2-diboraalkene **11** (*vide infra*). Reaction of **3** with <sup>10</sup>BuNC afforded <sup>10</sup>Bu-substituted 1,2,4,3-triazaborole derivative **12** in 16% isolated yield, whereas from the reactions with excess DippNC, PhNC, and 2,6-F<sub>2</sub>C<sub>6</sub>H<sub>3</sub>NC under the similar reaction conditions, 2-boranyl-indole derivatives **13** (21%), **14** (15%), and **15** (20%) were obtained respectively, after workup. The <sup>11</sup>B NMR chemical shifts were observed at 30.0 ppm (**12**), 28.9 ppm (**13**), 25.6 ppm (**14**), and 24.9 ppm (**15**). Products **12**–**15** were fully characterized by standard spectroscopic methods, including X-ray diffraction analysis (Figures 13–16).

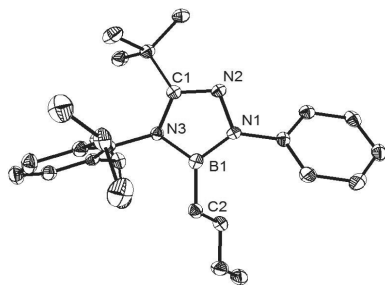


**Figure 13.** Molecular structure of **12** (all hydrogen atoms are omitted for clarity). Thermal ellipsoids are set at the 50% probability level.

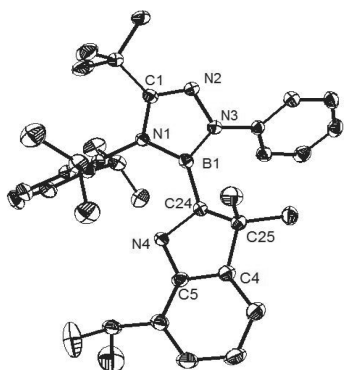


**Figure 14.** Molecular structure of **13** (all hydrogen atoms are omitted for clarity). Thermal ellipsoids are set at the 50% probability level.

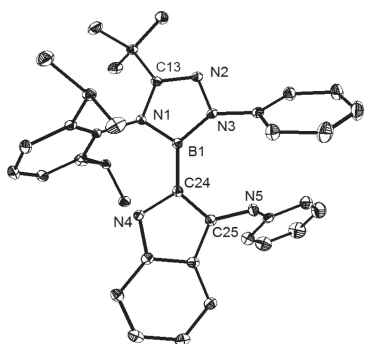


**Figure 15.** Molecular structure of **14** (all hydrogen atoms are omitted for clarity). Thermal ellipsoids are set at the 50% probability level.

Although considerable air and moisture sensitivities of compound **11** impeded the isolation, its chemical trapping with Me<sub>3</sub>SiCl successfully afforded diboradisiloxyalkene **11'** (6%), supporting the generation of lithium (*E*)-1,2-diboranyl-ethene-1,2-bis(olate) species **11** (Scheme 5, Figure 17). In this

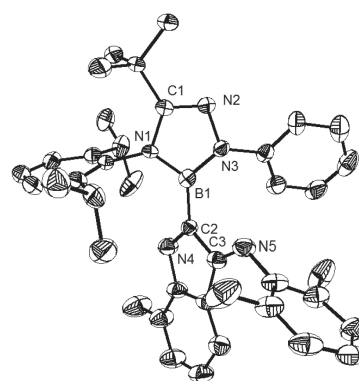
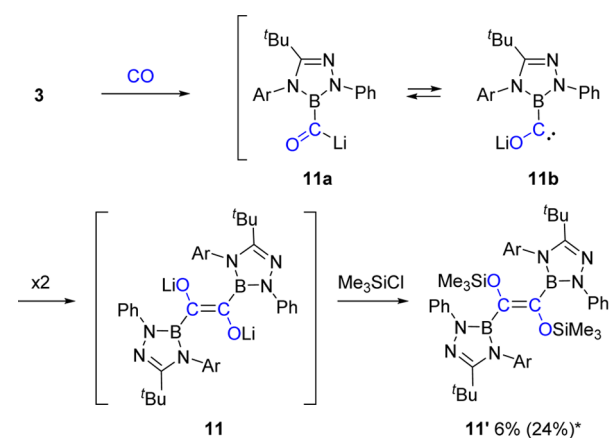


**Figure 16.** Molecular structure of **15** (all hydrogen atoms are omitted for clarity). Thermal ellipsoids are set at the 50% probability level.

**Scheme 5. Proposed Reaction Pathway for the Formation of **11** from **3** and CO and Its Trapping Reaction with Me<sub>3</sub>SiCl<sup>a\*</sup>**



<sup>a\*</sup> indicates NMR yield.

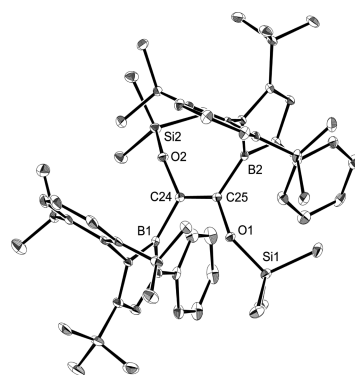


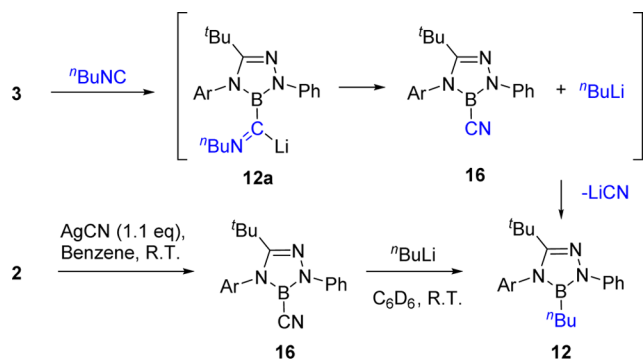
**Figure 17.** Molecular structure of **11'** (all hydrogen atoms are omitted for clarity). Thermal ellipsoids are set at the 50% probability level.

reaction, we could not observe any products from **11** via a Bora–Brook rearrangement, reported by Nozaki and Yamashita et al. very recently.<sup>31</sup> Putatively, compound **11** was formed via subsequent CO insertion into the B–Li bond in **3** to generate **11a** and isomerization to **11b** followed by dimerization. Note that analogous CO insertion into a C–Li bond and subsequent isomerization to alkoxy carbene and its dimerization for the formation of dilithiumdiolate species were proposed by Seyferth and Nudelman et al.,<sup>32</sup> in which the dilithiumdiolate intermediates were not spectroscopically detected, and its chemical trapping products were characterized only by IR, UV,

mass and  $^1\text{H}$  NMR spectra. To the best of our knowledge, formation of **11'** represents the first example for the synthesis of 1,2-diboranylene from boryllithium **3**.<sup>33</sup> We have also examined the reaction of CO with other borylmetals **5**, **6**, **8**, **9**, **10**, in all of which no reactions were observed, presumably due to the lower ionic nature of the B–M bonds in these borylmetals compared with the B–Li bond in **3**.

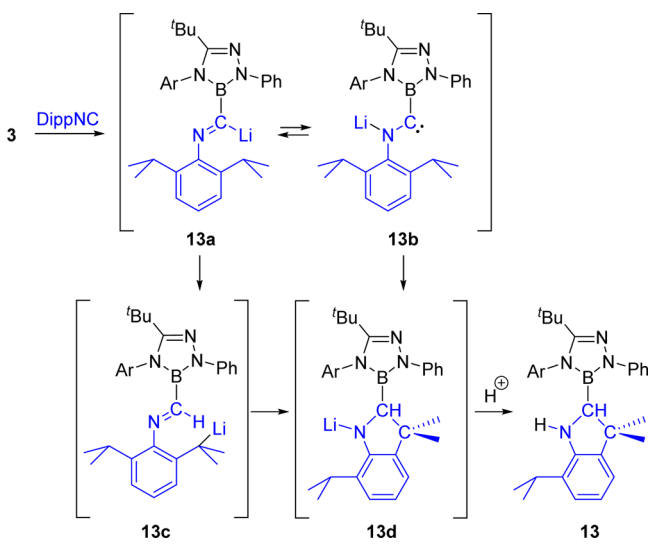
Based on the result of the reaction between **3** and CO, it is reasonable to envisage that the reactions of **3** with isocyanides may start from the insertion of the isocyanide carbon into the B–Li bond in **3**. With  $^n\text{BuNC}$ , spontaneous elimination of  $^n\text{BuLi}$  from the intermediate **12a** would yield a CN-substituted borole **16** which would react further with  $^n\text{BuLi}$  to afford **12** (Scheme 6). To confirm the proposed reaction mechanism, we

Scheme 6. Proposed Mechanism for the Formation of **12**



synthesized compound **16** by the reaction of **2** and AgCN and examined the reaction of **16** and  $^n\text{BuLi}$ , from which **12** was obtained in 77% NMR yield. In the reaction of **3** with DippNC, intermediate **13a** would abstract an acidic H atom in one of the  $^i\text{Pr}$  groups to generate benzyl lithium **13c** (Scheme 7).

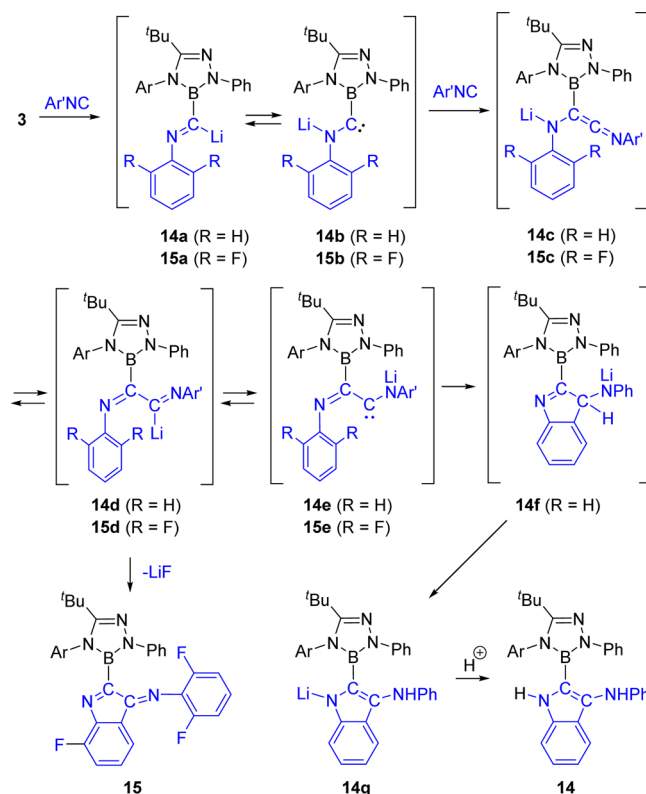
Scheme 7. Proposed Mechanism for the Formation of **13**



Subsequent intramolecular cyclization via nucleophilic attack by benzyl lithium to the imine moiety would form 2-boranylidoline derivative **13d**. Alternatively, isomerization of **13a** to carbene species **13b** followed by C–H bond insertion at the carbene center also could generate **13d**,<sup>27c,d,34</sup> which may be protonated during workup to afford **13**.

Similar to the generation of **11b** (Scheme 5), reactions of **3** with PhNC and 2,6-F<sub>2</sub>C<sub>6</sub>H<sub>3</sub>NC would yield aminoborylcarbene intermediates **14b/15b** via **14a/15a**, respectively (Scheme 8).

Scheme 8. Proposed Mechanism for the Formation of **14** and **15**



Carbene intermediates **14b/15b** would then be trapped by second isocyanides Ar'NC to render keteneimines **14c/15c**,<sup>35</sup> which is in contrast to the reaction with DippNC where addition of a second isocyanide did not occur for **13b** (Scheme 7), presumably due to the steric hindrance of the bulky Dipp group. Intermediate **14c/15c** could be in equilibrium with **14d/15d** and **14e/15e**. **14e** would undergo cyclization via an insertion of the carbene carbon to a C–H bond at the *ortho*-position in the Ph-group to form **14f**, from which subsequent isomerization to **14g** and protonation would give **14**. By contrast, intermediate **15e** did not undergo similar cyclization, probably due to the presence of the strong C–F bonds at the *ortho*-position in the Ph-ring. Instead, from **15d**, the intramolecular cyclization through S<sub>N</sub>Ar reaction would proceed along with the elimination of LiF to afford **15**.

To gain deep insight into the reaction mechanism, we carried out a further reaction employing S<sub>8</sub> to trap the carbene intermediate in the reaction of **3** and 2,6-F<sub>2</sub>C<sub>6</sub>H<sub>3</sub>NC. A mixture of freshly generated **3** and 2 equiv of 2,6-F<sub>2</sub>C<sub>6</sub>H<sub>3</sub>NC in THF was stirred at 0 °C for 30 min. Then, excess amounts of sulfur (S<sub>8</sub>) was added to the reaction mixture and stirred at room temperature overnight. After workup, compound **17** was obtained in low yield (7%), in addition to **15** (Scheme 9, Figure 18). Formation of **17** suggests that carbene intermediate **15e** would be involved in the reaction (Scheme 10). Oxidation of the carbene carbon in **15e** with sulfur to lead **17a** followed by a cyclization through S<sub>N</sub>Ar reaction would afford 3-boranylquinoxaline thione derivative **17**.



**Scheme 9. Trapping Reaction with  $S_8$  in the Reaction between 3 and 2,6-F<sub>2</sub>C<sub>6</sub>H<sub>3</sub>NC**

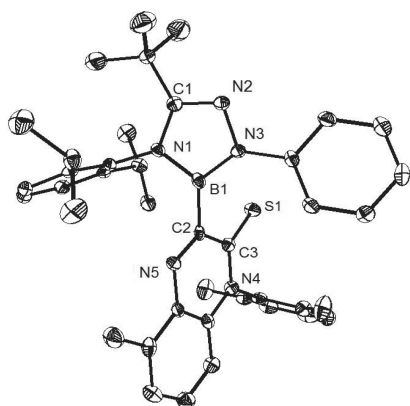
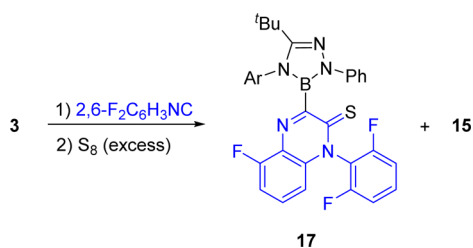
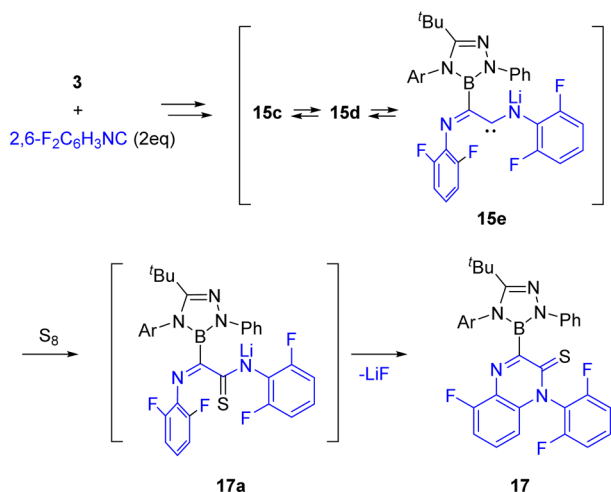


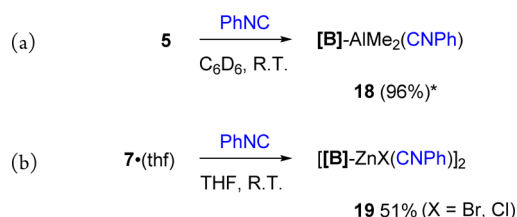
**Figure 18.** Molecular structure of 17 (all hydrogen atoms are omitted for clarity). Thermal ellipsoids are set at the 50% probability level.

**Scheme 10. Proposed Mechanism for the Formation of 17**



**Reactions between 1,2,4,3-Triazaborol-3-yl-metals 5–7 and Isonitriles.** We have also examined the reactions of borylmetals 5 (Al), 6 (Au), 7 (Zn), with PhNC. While 6 did not react with PhNC, treatment of compound 5 with PhNC underwent clean substitution of THF molecules by PhNC at the Al center to afford 18, as confirmed by <sup>1</sup>H, <sup>11</sup>B{<sup>1</sup>H}, <sup>13</sup>C, and <sup>27</sup>Al NMR spectroscopy (Scheme 11a). Product 18 is thermally stable at ambient temperature, but it decomposed quickly at 50 °C. Reaction of borylhalozinc 7·(thf) with PhNC afforded 19 (51%), which was unambiguously confirmed by X-ray diffraction analysis (Scheme 11b, Figure 19). These results suggest that the initial step of the reaction between borylmetals and isocyanides may be coordination of the isocyanide carbon to the metal center. Note that the reaction pathways proposed for

**Scheme 11. Reactions of Borylmetals 5 and 7·(thf) with PhNC<sup>a</sup>**



<sup>a</sup>\* indicates NMR yield.

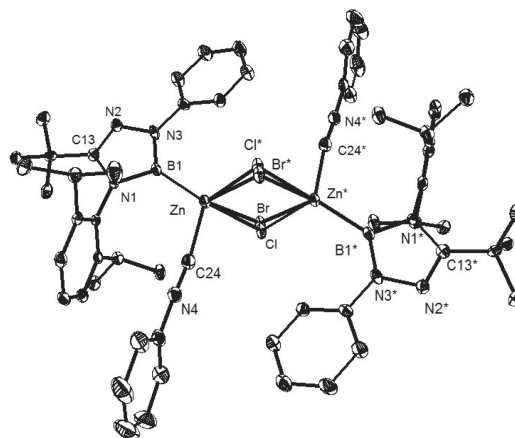
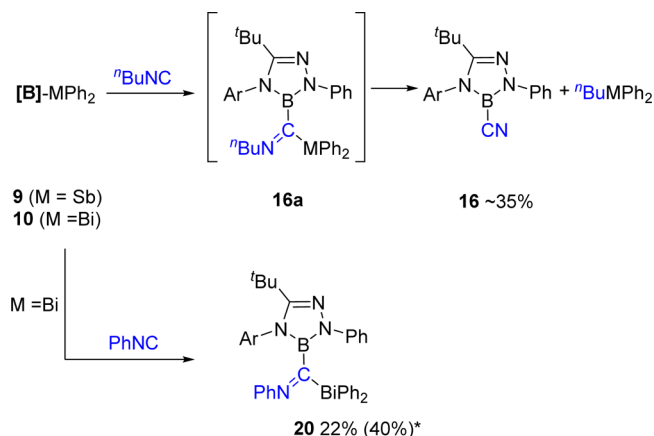


**Figure 19.** Molecular structure of 19 (all hydrogen atoms are omitted for clarity). Thermal ellipsoids are set at the 50% probability level.

the insertion reaction of isocyanides into boron–nonmetal bonds involve initial coordination of isocyanides to the boron center,<sup>27</sup> which is in marked contrast to our mechanism. We attempted heating 19 in a THF solution, which led to indiscernible complex mixtures, and thus no product via an insertion of PhNC to the B–Zn bond was obtained.

Interestingly, adding <sup>n</sup>BuNC to boryl-group 15 metals 9 and 10 led after workup to CN-substituted borole 16 (Scheme 12, Figure 20). Based on the previous observation (Scheme 6), compound 16 could be formed by subsequent insertion of the isocyanide carbon into the B–M (M = Sb, Bi) bond yielding the intermediates 16a and elimination of <sup>n</sup>BuMPh<sub>2</sub>. When we

**Scheme 12. Reactions of Borylmetals 9 and 10 with <sup>n</sup>BuNC<sup>a</sup>**



<sup>a</sup>\* indicates NMR yield.

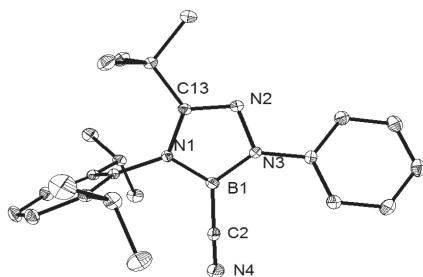


**Figure 20.** Molecular structure of **16** (all hydrogen atoms are omitted for clarity). Thermal ellipsoids are set at the 50% probability level.

employed PhNC, the reaction with **9** afforded a complex mixture, whereas in the reaction with **10**, a clean insertion of PhNC to the B–Bi bond of **10** took place, and **20** was obtained in 22% yield (Scheme 12, Figure 21). Note that these results

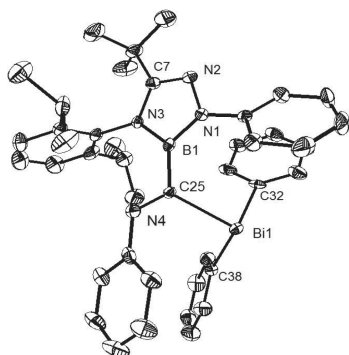


**Figure 21.** Molecular structure of **20** (all hydrogen atoms are omitted for clarity). Thermal ellipsoids are set at the 50% probability level.

document the first example demonstrating the reactivity of boron-group 15 metal bonds along with the bond activation. We also tried the similar reactions between compounds **9** and **10** with DippNC, but no reactions were confirmed even under heating condition, probably, the bulky Dipp-group encumbered the interaction between them.

## CONCLUSION

Ten years after the first isolation of boryllithium **I** by Segawa, Yamashita, and Nozaki group,<sup>2</sup> this report has demonstrated that 1,2,4,3-triazaborol-3-yl-lithium **3** can also be synthesized as isolable species. NMR spectroscopy, crystallographic analysis, and computational studies confirmed the considerable ionic nature of the B–Li bond in **3**. DFT calculation revealed that the B–Li bond in the parent 1,2,4,3-triazaborol-3-yl-lithium **opt-3'** is more polarized than that of the parent 1,3,2-diazaborol-3-yl-lithium **opt-I'**. Thus, it is indicated that the BCN<sub>3</sub> five-membered ring framework of 1,2,4,3-triazaborol-3-yl-lithium essentially enhances the ionic nature of the B–Li bond with respect to that with the BN<sub>2</sub>C<sub>2</sub> five-membered ring system. We showed that **3** exhibits nucleophilic nature and undergoes salt elimination reaction with various metal halides, which allowed access to a series of borylmetals including extremely rare boryl-group 15 metal compounds: [B]–AlMe<sub>2</sub>(thf) **5**, [B]–AuPPh<sub>3</sub> **6**, [[B]–ZnX(solv.)]<sub>2</sub> **7**, [B]–MgBr(thf)<sub>2</sub> **8**, [B]–MPh<sub>2</sub> (**9** M = Sb, **10** M = Bi). The reaction of **3** with CO followed by trapping with Me<sub>3</sub>SiCl confirmed the generation of lithium (*E*)-1,2-diboranylene-1,2-bis(olate) species **11**, which is in line with the works by Seyferth and Nudelman et al.<sup>32</sup> Investigation of

reactions between borylmetals **3**, **5–7**, **9**, **10** and various isonitriles disclosed the activity of B–M bonds significantly depends on the metals. Thus, it was found that the B–M bonds (M = Al, Au, Zn) in **5–7** were reluctant to react with isonitriles;<sup>36</sup> no reaction for **6** and replacement of THF molecules by isonitriles on the metal center were observed for **5** and **7**·(thf). Meanwhile, the B–Li bond in **3** and the B–Sb and B–Bi bonds in **9** and **10** were readily activated by the isonitrile carbon center. The former afforded a variety of 2-borylindole derivatives **13–15**, whereas the latter presented the first reaction involving the cleavage of the B–Sb and B–Bi single bonds. Formation of compounds **11** and **13–15** suggests that carbene intermediates are involved in those reactions. Indeed, addition of S<sub>8</sub> during the reaction of **3** with 2,6-F<sub>2</sub>C<sub>6</sub>H<sub>3</sub>NC afforded 3-boranyl-quinoxaline thione derivative **17**. We believe that the results from these systematic and comparative studies on 1,2,4,3-triazaborol-3-yl-metals will enhance the knowledge of the nature of the boron–metal bonds and allow to design novel isolable borylmetals, which are under active investigation in our laboratory.

## ASSOCIATED CONTENT

### Supporting Information

The Supporting Information is available free of charge on the ACS Publications website at DOI: 10.1021/jacs.6b03432.

Synthesis, NMR spectra, computational details including Cartesian coordinates for stationary points (PDF) crystallographic data (ZIP)

## AUTHOR INFORMATION

### Corresponding Author

\*rkinjo@ntu.edu.sg

### Notes

The authors declare no competing financial interest.

## ACKNOWLEDGMENTS

We are grateful to Nanyang Technological University and PSF/A\*STAR (SERC 1321202066) of Singapore for financial support.

## REFERENCES

- (1) (a) Yamashita, M.; Nozaki, K. In *Synthesis and Application of Organoboron Compounds*; Fernández, E., Whiting, A., Eds.; Springer International Publishing: Switzerland, 2015; p 1. (b) Mkhaid, I. A. I.; Barnard, J. H.; Marder, T. B.; Murphy, J. M.; Hartwig, J. F. *Chem. Rev.* **2010**, *110*, 890. (c) Hartwig, J. F. *Organotransition Metal Chemistry: From Bonding to Catalysis*; University Science Books: Sausalito, CA, 2010. (d) Braunschweig, H.; Dewhurst, R. D.; Schneider, A. *Chem. Rev.* **2010**, *110*, 3924. (e) Dang, L.; Lin, Z.; Marder, T. B. *Chem. Commun.* **2009**, 3987. (f) Kays, D. L.; Aldridge, S. *Struct. Bonding (Berlin)* **2008**, *130*, 29. (g) Aldridge, S.; Coombs, D. L. *Coord. Chem. Rev.* **2004**, *248*, 535. (h) Braunschweig, H.; Colling, M. *Coord. Chem. Rev.* **2001**, *223*, 1. (i) Irvine, G. J.; Lesley, M. J. G.; Marder, T. B.; Norman, N. C.; Rice, C. R.; Robins, E. G.; Roper, W. R.; Whittell, G. R.; Wright, L. J. *Chem. Rev.* **1998**, *98*, 2685. (j) Burgess, K.; Ohlmeyer, M. J. *Chem. Rev.* **1991**, *91*, 1179.
- (2) Segawa, Y.; Yamashita, M.; Nozaki, K. *Science* **2006**, *314*, 113.
- (3) (a) Dettenrieder, N.; Dietrich, H. M.; Schädle, C.; Maichle-Mössmer, C.; Törnroos, K. W.; Anwender, R. *Angew. Chem., Int. Ed.* **2012**, *51*, 4461. (b) Dettenrieder, N.; Hollfelder, C. O.; Jende, L. N.; Maichle-Mössmer, C.; Anwender, R. *Organometallics* **2014**, *33*, 1528. (c) Dettenrieder, N.; Schädle, C.; Maichle-Mössmer, C.; Sirsch, P.; Anwender, R. *J. Am. Chem. Soc.* **2014**, *136*, 886. (d) Protchenko, A. V.; Dange, D.; Harmer, J. R.; Tang, C. Y.; Schwarz, A. D.; Kelly, M. J.

- Phillips, N.; Tirfoin, R.; Birj Kumar, K. H.; Jones, C.; Kaltsoyannis, N.; Mountford, P.; Aldridge, S. *Nat. Chem.* **2014**, *6*, 315. (e) Protchenko, A. V.; Birj Kumar, K. H.; Dange, D.; Schwarz, A. D.; Vidovic, D.; Jones, C.; Kaltsoyannis, N.; Mountford, P.; Aldridge, S. *J. Am. Chem. Soc.* **2012**, *134*, 6500. (f) Protchenko, A. V.; Dange, D.; Schwarz, A. D.; Tang, C. Y.; Phillips, N.; Mountford, P.; Jones, C.; Aldridge, S. *Chem. Commun.* **2014**, *50*, 3841. (g) Saleh, L. M. A.; Birj Kumar, K. H.; Protchenko, A. V.; Schwarz, A. D.; Aldridge, S.; Jones, C.; Kaltsoyannis, N.; Mountford, P. *J. Am. Chem. Soc.* **2011**, *133*, 3836. (h) Segawa, Y.; Yamashita, M.; Nozaki, K. *Angew. Chem., Int. Ed.* **2007**, *46*, 6710. (i) Frank, R.; Howell, J.; Tirfoin, R.; Dange, D.; Jones, C.; Mingos, D. M. P.; Aldridge, S. *J. Am. Chem. Soc.* **2014**, *136*, 15730. (j) Arnold, T.; Braunschweig, H.; Ewing, W. C.; Kramer, T.; Mies, J.; Schuster, J. K. *Chem. Commun.* **2015**, *51*, 737. (k) Terabayashi, T.; Kajiwara, T.; Yamashita, M.; Nozaki, K. *J. Am. Chem. Soc.* **2009**, *131*, 14162. (l) Frank, R.; Howell, J.; Campos, J.; Tirfoin, R.; Phillips, N.; Zahn, S.; Mingos, D. M. P.; Aldridge, S. *Angew. Chem., Int. Ed.* **2015**, *54*, 9586. (m) Protchenko, A. V.; Blake, M. P.; Schwarz, A. D.; Jones, C.; Mountford, P.; Aldridge, S. *Organometallics* **2015**, *34*, 2126. (n) Protchenko, A. V.; Blake, J. I.; Saleh, L. M. A.; Blake, M. P.; Schwarz, A. D.; Kolychev, E. L.; Thompson, A. L.; Jones, C.; Mountford, P.; Aldridge, S. *J. Am. Chem. Soc.* **2016**, *138*, 4555.
- (4) (a) Segawa, Y.; Suzuki, Y.; Yamashita, M.; Nozaki, K. *J. Am. Chem. Soc.* **2008**, *130*, 16069. See also: (b) Yamashita, M.; Nozaki, K. *Yuki Gosei Kagaku Kyokaiishi* **2010**, *68*, 359. (c) Yamashita, M. *Bull. Chem. Soc. Jpn.* **2011**, *84*, 983.
- (5) (a) Yamashita, M.; Suzuki, Y.; Segawa, Y.; Nozaki, K. *J. Am. Chem. Soc.* **2007**, *129*, 9570. (b) Yamashita, M.; Nozaki, K. *Bull. Chem. Soc. Jpn.* **2008**, *81*, 1377.
- (6) (a) Kajiwara, T.; Terabayashi, T.; Yamashita, M.; Nozaki, K. *Angew. Chem., Int. Ed.* **2008**, *47*, 6606. (b) Okuno, Y.; Yamashita, M.; Nozaki, K. *Angew. Chem., Int. Ed.* **2011**, *50*, 920. (c) Okuno, Y.; Yamashita, M.; Nozaki, K. *Eur. J. Org. Chem.* **2011**, *2011*, 3951. See also: (d) Campos, J.; Aldridge, S. *Angew. Chem., Int. Ed.* **2015**, *54*, 14159.
- (7) (a) Braunschweig, H.; Chiu, C.-W.; Radacki, K.; Kupfer, T. *Angew. Chem., Int. Ed.* **2010**, *49*, 2041. (b) Braunschweig, H.; Chiu, C.-W.; Kupfer, T.; Radacki, K. *Inorg. Chem.* **2011**, *50*, 4247. (c) Bertermann, R.; Braunschweig, H.; Dewhurst, R. D.; Hörl, C.; Kramer, T.; Krummenacher, I. *Angew. Chem., Int. Ed.* **2014**, *53*, 5453.
- (8) (a) Laitar, D. S.; Müller, P.; Sadighi, J. P. *J. Am. Chem. Soc.* **2005**, *127*, 17196. See also: (b) Takahashi, K.; Ishiyama, T.; Miyaura, N. *J. Organomet. Chem.* **2001**, *625*, 47.
- (9) (a) Braunschweig, H.; Burzler, M.; Dewhurst, R. D.; Radacki, K. *Angew. Chem., Int. Ed.* **2008**, *47*, 5650. (b) Braunschweig, H.; Brenner, P.; Dewhurst, R. D.; Kaupp, M.; Müller, R.; Östreicher, S. *Angew. Chem., Int. Ed.* **2009**, *48*, 9735. (c) Braunschweig, H.; Damme, A.; Dewhurst, R. D.; Kramer, T.; Östreicher, S.; Radacki, K.; Vargas, A. *J. Am. Chem. Soc.* **2013**, *135*, 2313. (d) Bertermann, R.; Braunschweig, H.; Ewing, W. C.; Kramer, T.; Phukan, A. K.; Vargas, A.; Werner, C. *Chem. Commun.* **2014**, *50*, 5729.
- (10) (a) Bernhardt, E.; Bernhardt-Pitchougina, V.; Willner, H.; Ignatiev, N. V. *Angew. Chem., Int. Ed.* **2011**, *50*, 12085. (b) Landmann, J.; Sprenger, J. A. P.; Bertermann, R.; Ignat'ev, N.; Bernhardt-Pitchougina, V.; Bernhardt, E.; Willner, H.; Finze, M. *Chem. Commun.* **2015**, *51*, 4989.
- (11) Ruiz, D. A.; Ung, G.; Melaimi, M.; Bertrand, G. *Angew. Chem., Int. Ed.* **2013**, *52*, 7590.
- (12) Selected examples: (a) Dettenrieder, N.; Aramaki, Y.; Wolf, B. M.; Maichle-Mössmer, C.; Zhao, X.; Yamashita, M.; Nozaki, K.; Anwander, R. *Angew. Chem., Int. Ed.* **2014**, *53*, 6259. (b) Hayashi, Y.; Segawa, Y.; Yamashita, M.; Nozaki, K. *Chem. Commun.* **2011**, *47*, 5888. (c) Nozaki, K.; Aramaki, Y.; Yamashita, M.; Ueng, S.-H.; Malacria, M.; Lacôte, E.; Curran, D. P. *J. Am. Chem. Soc.* **2010**, *132*, 11449. (d) Monot, J.; Solovyev, A.; Bonin-Dubarle, H.; Derat, É.; Curran, D. P.; Robert, M.; Fensterbank, L.; Malacria, M.; Lacôte, E. *Angew. Chem., Int. Ed.* **2010**, *49*, 9166. (e) Weber, L. *Eur. J. Inorg. Chem.* **2012**, *2012*, 5595. See also: (f) Segawa, Y.; Yamashita, M.; Nozaki, K. *J. Am. Chem. Soc.* **2009**, *131*, 9201. (g) Segawa, Y.; Yamashita, M.; Nozaki, K. *Organometallics* **2009**, *28*, 6234.
- (13) Scott, N. M.; Nolan, S. P. *Eur. J. Inorg. Chem.* **2005**, *2005*, 1815.
- (14) (a) Flanigan, D. M.; Romanov-Michailidis, F.; White, N. A.; Rovis, T. *Chem. Rev.* **2015**, *115*, 9307. (b) Hopkinson, M. N.; Richter, C.; Schedler, M.; Glorius, F. *Nature* **2014**, *510*, 485. (c) Maji, B.; Breugst, M.; Mayr, H. *Angew. Chem., Int. Ed.* **2011**, *50*, 6915. (d) Enders, D.; Breuer, K.; Raabe, G.; Runsink, J.; Teles, J. H.; Melder, J.-P.; Ebel, K.; Brode, S. *Angew. Chem., Int. Ed. Engl.* **1995**, *34*, 1021. (e) Arduengo, A. J., III; Harlow, R. L.; Kline, M. *J. Am. Chem. Soc.* **1991**, *113*, 361.
- (15) Loh, Y.-K.; Chong, C.-C.; Ganguly, R.; Li, Y.; Vidovic, D.; Kinjo, R. *Chem. Commun.* **2014**, *50*, 8561.
- (16) Cordero, B.; Gomez, V.; Platero-Prats, A. E.; Reves, M.; Echeverria, J.; Cremades, E.; Barragan, F.; Alvarez, S. *Dalton Trans.* **2008**, 2832.
- (17) Dange, D.; Davey, A.; Abdalla, J. A. B.; Aldridge, S.; Jones, C. *Chem. Commun.* **2015**, *51*, 7128.
- (18) (a) Baenziger, N. C.; Bennett, W. E.; Soboroff, D. M. *Acta Crystallogr., Sect. B: Struct. Crystallogr. Cryst. Chem.* **1976**, *32*, 962. (b) Gavens, P. D.; Guy, J. J.; Mays, M. J.; Sheldrick, G. M. *Acta Crystallogr., Sect. B: Struct. Crystallogr. Cryst. Chem.* **1977**, *33*, 137. (c) Hong, X.; Cheung, K. K.; Guo, C. X.; Che, C. M. *J. Chem. Soc., Dalton Trans.* **1994**, 1867.
- (19) (a) Lube, M. S.; Wells, R. L.; White, P. S. *J. Chem. Soc., Dalton Trans.* **1997**, 285. (b) Jasper, S. A., Jr; Roach, S.; Stipp, J. N.; Huffman, J. C.; Todd, L. J. *Inorg. Chem.* **1993**, *32*, 3072.
- (20) Marquardt, C.; Hegen, O.; Hautmann, M.; Balázs, G.; Bodensteiner, M.; Virovets, A. V.; Timoshkin, A. Y.; Scheer, M. *Angew. Chem., Int. Ed.* **2015**, *54*, 13122.
- (21) Adams, E. A.; Kolis, J. W.; Pennington, W. T. *Acta Crystallogr., Sect. C: Cryst. Struct. Commun.* **1990**, *46*, 917.
- (22) (a) Arduengo, A. J., III; Krafczyk, R.; Schmutzler, R.; Craig, H. A.; Goerlich, J. R.; Marshall, W. J.; Unverzagt, M. *Tetrahedron* **1999**, *55*, 14523. (b) Arduengo, A. J., III; Goerlich, J. R.; Marshall, W. J. *J. Am. Chem. Soc.* **1995**, *117*, 11027. (c) Korotkikh, N. I.; Raenko, G. F.; Pekhtereva, T. M.; Shvaika, O. P.; Cowley, A. H.; Jones, J. N. *Russ. J. Org. Chem.* **2006**, *42*, 1822.
- (23) (a) Murai, S.; Iwamoto, K. In *Modern Carbonyl Chemistry*; Otera, J., Ed.; Wiley-VCH: Weinheim, Germany, 2000; p 131. (b) Colquhoun, H. M.; Thompson, D. J.; Twigg, M. V. *Carbonylation-Direct Synthesis of Carbonyl Compounds*; Plenum: New York, 1991. (c) Wakefield, B. J. *Organolithium Methods*; Academic Press: San Diego, 1988; p 95. (d) Narayana, C.; Periasamy, M. *Synthesis* **1985**, 1985, 253. (e) Seyferth, D.; Weinstein, R. M.; Wang, W.; Hui, R. C.; Archer, C. M. *Isr. J. Chem.* **1984**, *24*, 167.
- (24) For examples of CO insertion into the B–E bond, see: (a) Asakawa, H.; Lee, K.-H.; Lin, Z.; Yamashita, M. *Nat. Commun.* **2014**, *5*, 4245. (b) Braunschweig, H.; Dellermann, T.; Dewhurst, R. D.; Ewing, W. C.; Hammond, K.; Jimenez-Halla, J. O. C.; Kramer, T.; Krummenacher, I.; Mies, J.; Phukan, A. K.; Vargas, A. *Nat. Chem.* **2013**, *5*, 1025. (c) Sajid, M.; Elmer, L.-M.; Rosorius, C.; Daniliuc, C. G.; Grimme, S.; Kehr, G.; Erker, G. *Angew. Chem., Int. Ed.* **2013**, *52*, 2243. (d) Teichmann, J.; Stock, H.; Pritzkow, H.; Siebert, W. *Eur. J. Inorg. Chem.* **1998**, *1998*, 459. (e) Paetzold, P.; Redenz-Stormanns, B.; Boese, R. *Angew. Chem., Int. Ed. Engl.* **1990**, *29*, 900. (f) Brown, H. C. *Acc. Chem. Res.* **1969**, *2*, 65. See also: (g) Dobrovetsky, R.; Stephan, D. W. *J. Am. Chem. Soc.* **2013**, *135*, 4974. (h) Braunschweig, H.; Celik, M. A.; Dewhurst, R. D.; Kachel, S.; Wennemann, B. *Angew. Chem., Int. Ed.* **2016**, *55*, 5076.
- (25) (a) Wang, B.; Kang, X.; Nishiura, M.; Luo, Y.; Hou, Z. *Chem. Sci.* **2016**, *7*, 803. (b) Li, S.; Cheng, J.; Chen, Y.; Nishiura, M.; Hou, Z. *Angew. Chem., Int. Ed.* **2011**, *50*, 6360.
- (26) (a) Boyarskiy, V. P.; Bokach, N. A.; Luzyanin, K. V.; Kukushkin, V. Y. *Chem. Rev.* **2015**, *115*, 2698. (b) Mironov, M. A. In *Isocyanide Chemistry*; Wiley-VCH Verlag GmbH & Co. KGaA: Weinheim, Germany, 2012; pp 35–73.
- (27) (a) Barnett, B. R.; Moore, C. E.; Rheingold, A. L.; Figueroa, J. S. *Chem. Commun.* **2015**, *51*, 541. (b) Barnett, B. R.; Moore, C. E.;

Rheingold, A. L.; Figueroa, J. S. *J. Am. Chem. Soc.* **2014**, *136*, 10262. (c) Sugimoto, M.; Fukuda, T.; Nakamura, H.; Ito, Y. *Organometallics* **2000**, *19*, 719. (d) Sugimoto, M.; Fukuda, T.; Ito, Y. *J. Organomet. Chem.* **2002**, *643*, 508. (e) Meller, A.; Batka, H. *Monatsh. Chem.* **1970**, *101*, 648. (f) Meller, A.; Batka, H. *Monatsh. Chem.* **1969**, *100*, 1823. See also: (g) Böhnke, J.; Braunschweig, H.; Dellermann, T.; Ewing, W. C.; Kramer, T.; Krummenacher, I.; Vargas, A. *Angew. Chem., Int. Ed.* **2015**, *54*, 4469.

(28) (a) Braunschweig, H.; Dewhurst, R. D.; Hupp, F.; Nutz, M.; Radacki, K.; Tate, C. W.; Vargas, A.; Ye, Q. *Nature* **2015**, *522*, 327. (b) Braunschweig, H.; Ewing, W. C.; Ferkinghoff, K.; Hermann, A.; Kramer, T.; Shang, R.; Siedler, E.; Werner, C. *Chem. Commun.* **2015**, *51*, 13032. (c) Braunschweig, H.; Radacki, K.; Shang, R.; Tate, C. W. *Angew. Chem., Int. Ed.* **2013**, *52*, 729. (d) Braunschweig, H.; Herbst, T.; Radacki, K.; Tate, C. W.; Vargas, A. *Chem. Commun.* **2013**, *49*, 1702.

(29) Tobisu, M.; Fujihara, H.; Koh, K.; Chatani, N. *J. Org. Chem.* **2010**, *75*, 4841.

(30) Braunschweig, H.; Ewing, W. C.; Ferkinghoff, K.; Hermann, A.; Kramer, T.; Shang, R.; Siedler, E.; Werner, C. *Chem. Commun.* **2015**, *51*, 13032.

(31) Kisu, H.; Sakaino, H.; Ito, F.; Yamashita, M.; Nozaki, K. *J. Am. Chem. Soc.* **2016**, *138*, 3548.

(32) (a) Seyferth, D.; Weinstein, R. M. *J. Am. Chem. Soc.* **1982**, *104*, 5534. (b) Seyferth, D.; Weinstein, R. M.; Wang, W. *J. Org. Chem.* **1983**, *48*, 1144. (c) Weinstein, R. M.; Wang, W.; Seyferth, D. *J. Org. Chem.* **1983**, *48*, 3367. (d) Seyferth, D.; Weinstein, R. M.; Wang, W.; Hui, R. C. *Tetrahedron Lett.* **1983**, *24*, 4907. (e) Seyferth, D.; Hui, R. C. *Tetrahedron Lett.* **1984**, *25*, 2623. (f) Seyferth, D.; Wang, W.; Hui, R. C. *Tetrahedron Lett.* **1984**, *25*, 1651. (g) Seyferth, D.; Hui, R. C. *J. Org. Chem.* **1985**, *50*, 1985. (h) Seyferth, D.; Hui, R. C. *J. Am. Chem. Soc.* **1985**, *107*, 4551. (i) Seyferth, D.; Hui, R. C.; Wang, W.; Archer, C. M. *J. Org. Chem.* **1993**, *58*, 5843. (j) Nudelman, N. S.; Vitale, A. A. *J. Org. Chem.* **1981**, *46*, 4625. (k) Nudelman, N. S.; Outumuro, P. *J. Org. Chem.* **1982**, *47*, 4347. The reaction of PhLi and CO followed by the trapping with acetic anhydride afforded only cis-product, which is in sharp contrast to our result (Figure 17). For the detail, see: (l) Nudelman, N. S.; Vitale, A. A. *J. Organomet. Chem.* **1983**, *241*, 143. (m) Perez, D.; Nudelman, N. S. *J. Org. Chem.* **1988**, *53*, 408. (n) Nudelman, N. S.; Doctorovich, F. *Tetrahedron* **1994**, *50*, 4651.

(33) (a) Morken, J. P. *Comprehensive Organic Synthesis*, 2nd ed.; John Wiley and Sons, Inc.: New York, 2014; Vol. 4, p 939. (b) Takaya, J.; Iwasawa, N. *ACS Catal.* **2012**, *2*, 1993. (c) Shimizu, M.; Hiyama, T. *Proc. Jpn. Acad., Ser. B* **2008**, *84*, 75.

(34) Frey, G. D.; Masuda, J. D.; Donnadiou, B.; Bertrand, G. *Angew. Chem., Int. Ed.* **2010**, *49*, 9444.

(35) (a) Despagnet-Ayoub, E.; Gornitzka, H.; Bourissou, D.; Bertrand, G. *Eur. J. Org. Chem.* **2003**, *2003*, 2039. (b) Merceron, N.; Miqueu, K.; Baceiredo, A.; Bertrand, G. *J. Am. Chem. Soc.* **2002**, *124*, 6806. (c) Amsallem, D.; Mazières, S.; Piquet-Fauré, V.; Gornitzka, H.; Baceiredo, A.; Bertrand, G. *Chem. - Eur. J.* **2002**, *8*, 5305. (d) Solé, S.; Gornitzka, H.; Schoeller, W. W.; Bourissou, D.; Bertrand, G. *Science* **2001**, *292*, 1901.

(36) The reactions of **6** with Lewis acids such as BH<sub>3</sub>, BX<sub>3</sub>, MeOTf, and additional AuCl were attempted. However, we could not observe the coordination of the backbone nitrogen atom to those Lewis acids.